

COLOR IMAGE COMPRESSION USING RIDGELET TRANSFORM AND SPIHT QUANTIZATION IMAGE VIDEO ⁺

ضغط الصورة الفيديوية الملونة باستخدام Ridgelet Transform وتكميمها باستخدام SPIHT

Walid A.Mahmoud *

Seham Ahmed Al-Musewy **

Rafah Abdul Hadi**

Abstract:

An effective image coding technique which involves transforming the image into another domain with Ridgelet function and then quantizing the coefficients with modified threshold. Ridgelet functions are effective in representing functions that have discontinuities along straight lines. Normal Wavelet transforms fail to represent such functions effectively. This paper shows the application of wavelet analysis to image compression. All of the four steps in compression namely transform, quantization, and coding, achieved quantization part deals with the translation of large set of data into a smaller set. On the other hand, coding deal with the representation of these transformed and quantized data into bits. A complete implementation, with remarkable results, are presented. The results obtained from the combination of ridgelet gave much better performance than that obtained from the Wavelet, and multiwavelet Transform with ridgelet transforms.

Keywords: image compression, wavelet transform, multiwavelet transform Color space, Color Image

المستخلص:

ان كفاءة تقنية تشفير الصورة تتضمن تحويل الصورة الى مجال اخر (Ridgelet Function) مع تكميم وتعديل المعاملات التي تتمثل باستمرار على خط مستقيم . فشل تحويل Wavelet transforms في تمثيل كفاءة الدوال. هذا البحث بين تطبيق لتحليلات Wavelet لضغط الصورة الفيديوية الملونة. وتحقيق اربعة مراحل لضغط وتحويل وتكميم جزء التكميم يتعامل مع ارسال مجموعة كبيرة من البيانات في مجموعة صغيرة بالاضافة الى ان التشفير يتعامل مع تكميم وتحويل البيانات من حيث Bit .
وتم الحصول على خوارزمية ضغط الصورة بنيت على تقنية ترميز فعال والذي يتضمن تكميم معاملات التحويل (Set Partitioning in Hierarchical Tree) تقسيم الترتيب في اشجار هرمية. ان هذا التنفيذ يظهر ان ضغط الصورة باستخدام عملية التحويل الهجين هو افضل كثيراً من الضغط باستخدام التحويل المفرد (Wavelet & multiwavelet Transform with ridgelet transforms).

Compression Techniques:

In general there are two compression techniques namely lossless and lossy compression.

1 Lossless compression:

One field where lossless compression is widely used is in digital medical imaging such as radiology. With the advent of major medical imaging techniques including: computed tomography (CT), magnetic resonance imaging (MRI), ultrasonography (US), etc., the need

⁺ Received on 25/11/2008 , Accepted on 10/2/2010 .

* Prof / Engineering college /Baghdad university .

** Lecturer-Foundation of Technical Education .

for efficient storage of terabits (Tb) of medical data and the demand for its transmission has necessitated the use of compression[1] .

2 Lossy compression

Contains degradation relative to the original. Often this is because the compression scheme completely discards redundant information. However, lossy schemes are capable of achieving much higher compression. Under normal viewing conditions, no visible loss is perceived (visually lossless) [2,3].

Image Transformation

The algorithm that describes the operation of the proposed image compression is shown in figure (1). Images are mostly acquired and display in the *RGB* color space. Unfortunately, the *R, G and B* components are highly correlated, therefore their straightforward encoding is not efficient. The technique consists in rough decorrelation obtained by liner color transformation from the *RGB* color space to the *Y C_r C_b* color space or to another similar space [4] .

The image compression parameter section and performance evaluation

Before the application of the proposed model, the basic parameters of the image compression can be estimated. The parameters that determine the performance of the image compression are image size, color resolutions, prim number, number of frame, level number. Here it is assumed that each input color image is originally represented in the *RGB* color space, and then converted into the *Y C_r C_b* color space for compression. When an input color image in the *Y C_r C_b* color space is obtained, it is necessary to determine a set of generalized transforms for the color image [5].

Compressions using the ridgelet transform, wavelet transform and multiwavelet transforms, and then converted back into the *RGB* space as the image for display. The compression ratio was also increased with an increased in threshold.

1 Multiwavelets Transform Computation: Basic Principles

For notational convenience, the set of scaling functions can be written using the vector notation.

$$\Phi(t) \equiv [\phi_1(t)\phi_2(t).....\phi_r(t)^T] \dots\dots\dots(1)$$

$\Phi(t)$ is called the multiscaling function. Likewise,

The multiwavelet function is defined from the set of wavelet functions as

$$\Psi(t) \equiv [\psi_1(t)\psi_2(t).....\psi_r(t)^T] \dots\dots\dots(2)$$

When $r = 1$, $\Psi(t)$ is called a scalar wavelet, or simply wavelet. While in principle r can be arbitrarily large. The multiwavelets studied to data are primarily for $r = 2$

The multiwavelet two- scale equations resemble those for scalar wavelets

$$\Phi(t) = \sqrt{2} \sum_{k=-\infty}^{\infty} H_k \Phi(2t - k) \dots\dots\dots(3)$$

$$\Psi(t) = \sqrt{2} \sum_{k=-\infty}^{\infty} G_k \Phi(2t - k) \quad \dots\dots\dots(4)$$

Note, however, that $\{H_k\}$ and $\{G_k\}$ are matrix filters. H_k and G_k are $r \times r$ matrices for each integer k . The filter bank representation is also mostly unchanged, except now the input and output of every branch in the multiffilter bank is a vector. A particular signal of interest, $x(t) \in V_0$, can be written as a linear combination of the basis functions $\{\phi_i(t - k)\}$

For computing discrete multiwavelet transform, scalar wavelet transform matrices can be written as follows:

$$W = \begin{bmatrix} H_0 & H_1 & H_2 & H_3 & 0 & 0 & \dots & 0 & 0 & 0 & 0 \\ 0 & 0 & H_0 & H_1 & H_2 & H_3 & \dots & 0 & 0 & 0 & 0 \\ \vdots & \vdots & \vdots & \vdots & \vdots & \vdots & \dots & \vdots & \vdots & \vdots & \vdots \\ H_2 & H_3 & 0 & 0 & 0 & 0 & \dots & 0 & 0 & H_0 & H_1 \\ G_0 & G_1 & G_2 & G_3 & 0 & 0 & \dots & 0 & 0 & 0 & 0 \\ 0 & 0 & G_0 & G_1 & G_2 & G_3 & \dots & 0 & 0 & 0 & 0 \\ \vdots & \vdots & \vdots & \vdots & \vdots & \vdots & \dots & \vdots & \vdots & \vdots & \vdots \\ 0 & 0 & 0 & 0 & 0 & 0 & \dots & G_0 & G_1 & G_2 & G_3 \\ G_2 & G_3 & 0 & 0 & 0 & 0 & \dots & 0 & 0 & G_0 & G_1 \end{bmatrix} \quad \dots\dots\dots(5)$$

Where H_i and G_i are the low and high- pass filter impulse responses. They are 2×2 matrices. By examining the transform matrices of the scalar wavelet equations and multiwavelet transform domain there are first and second high pass filter coefficients rather than one lowpass coefficient followed by one highpass coefficient such as in. Therefore, if these four coefficients are separated, there are four subbands in the transform domain [6,7] .

Multiwavelets have two or more scaling functions and mother wavelet for signal representation. The scaling and mother wavelet functions of the GHM filter. To implement the multiwavelet transform; we require a new filter bank structure where the low pass and highpass filter bank are matrices rather than scalars. That is. The two scaling and wavelet functions satisfy the following two-scale dilation equations[8].

$$\begin{bmatrix} \phi_1(t) \\ \phi_2(t) \end{bmatrix} = \sqrt{2} \sum_k H_k \begin{bmatrix} \phi_1(2t - k) \\ \phi_2(2t - k) \end{bmatrix} \quad \dots\dots\dots(6)$$

$$\begin{bmatrix} \psi_1(t) \\ \psi_2(t) \end{bmatrix} = \sqrt{2} \sum_k G_k \begin{bmatrix} \psi_1(2t - k) \\ \psi_2(2t - k) \end{bmatrix} \quad \dots\dots\dots(7)$$

$$H_1 = \sqrt{2} \begin{bmatrix} 3/10 & 0 \\ 9\sqrt{2}/40 & 1/2 \end{bmatrix} \quad \dots\dots\dots(8)$$

$$H_2 = \sqrt{2} \begin{bmatrix} 0 & 0 \\ 9\sqrt{2}/40 & -3/20 \end{bmatrix} \quad H_3 = \sqrt{2} \begin{bmatrix} 0 & 0 \\ -\sqrt{2}/40 & 0 \end{bmatrix}$$

And

$$G_0 = \sqrt{2} \begin{bmatrix} -\sqrt{2}/40 & -3/20 \\ -1/20 & -3\sqrt{2}/20 \end{bmatrix} \quad G_1 = \sqrt{2} \begin{bmatrix} 9\sqrt{2}/40 & -1/2 \\ 9/20 & 0 \end{bmatrix}$$

.....(9)

$$G_2 = \sqrt{2} \begin{bmatrix} 9\sqrt{2}/40 & -3/20 \\ -9/20 & -3\sqrt{2}/20 \end{bmatrix} \quad G_3 = \sqrt{2} \begin{bmatrix} -\sqrt{2}/40 & 0 \\ 1/20 & 0 \end{bmatrix}$$

2 Computation of FDMWT for 2-D Signal

The choice of the transform to be used depends on a number of factors, in particular, computational complexity and coding gain. Computation complexity is measured in terms of the number of multiplications and additions required for the implementation of the transform. Coding gain is a measure of how well the transformation compacts signal energy into a small number of coefficients. There are two main types of methods for computing discrete multiwavelet transform (DMWT) for 2-D signals which are separable and non- separable algorithms.

3 Computation of fast discrete multiwavelet transform (FDMWT) for Signal using

Separable Method

To compute a signal-level 2-D discrete multiwavelet transform using separable method, the next steps should be followed:

1. Checking input dimensions: input matrix should be of the length $N \times N$, where N must be power of two.
2. Constructing a transformation matrix W using GHM low and high pass filters matrices given in eqs (7) and (8)
3. Preprocessing row :doubles the number of the input matrix rows. So if the 2-D input is $N \times N$ matrix elements, after row preprocessing the same original matrix. The odd rows values, while the even rows are the original signal rows values multiplied

The Main Block Diagram of the Compression Method:

The main Block diagram of the encoded proposed compression method using hybrid transforms is given in Figure (1). It consists of the preprocessing which is dedicated to the selection of input image and its conversion into gray scale. Next, the hybrid transform will be applied. Then, the SPIHT will be performed on the resulted coefficients of the hybrid transform. It is them subjected to the run length coding algorithm, as well as a sort of coding

namely the Huffman code which will be applied to get the final coded image shown in Figure (1).

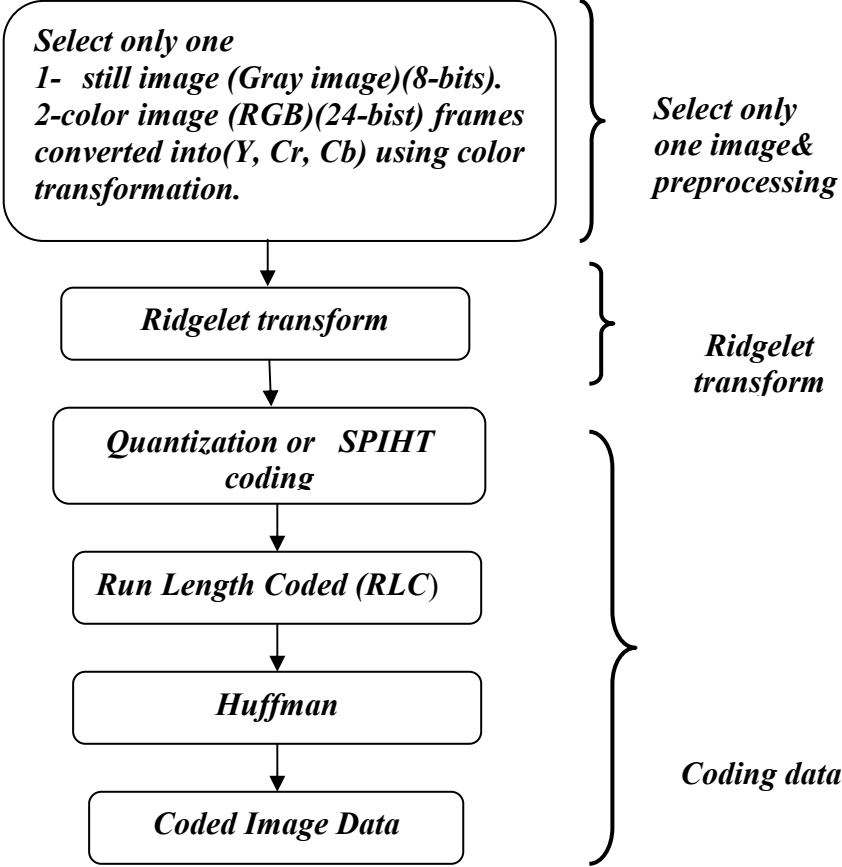


Figure (1) Block diagram of the proposed Image compression using hybrid transform (coded)

The proposed decoded method of decompression is given in Figure (2) it consists of the reverse operations of the encoding compression given before.

It starts with getting the decoded image data and applies Huffman decoding to it. The inverse of Run length will be applied. Next, it is required to apply the dequantization of SPIHT operations.

As a major operation it requires further the application of inverse Ridgelet transform. Finally, the reconstruction of the still image into its color transformation will be applied.

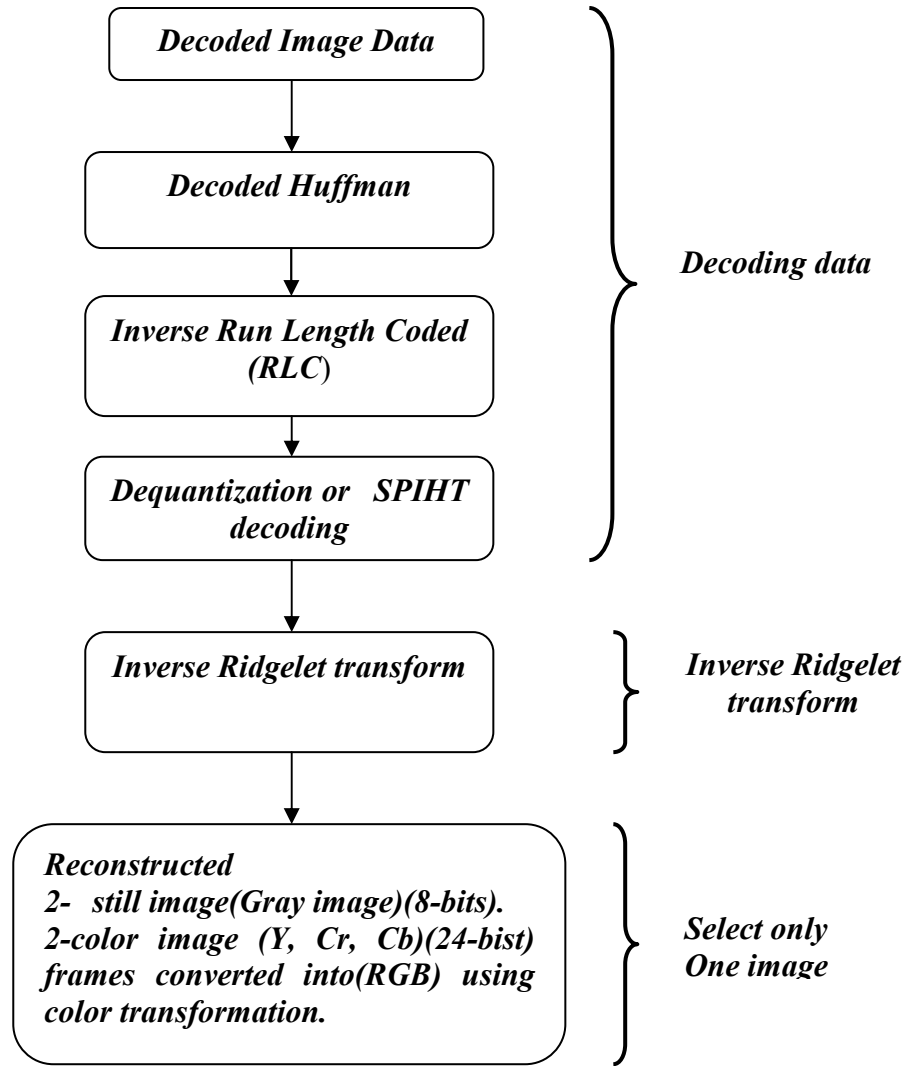


Figure (2) Block Diagram of The Proposed Image Compression Using Hybrid Transform (Decoded)

1- The Preprocessing of The Compression

As mentioned before the first operation in this compression method is the preprocessing. It is first required to convert the RGB image to Y, C_r, and C_b color space. the YC_rC_b is a subset of YUV that scales and shifts the chrominance values into the range of 0 to 1. The linear transform from RGB to YC_rC_b generates one luminance space Y and two chrominance (C_r and C_b) spaces. The chroma signals, C_r and C_b, are scaled versions of the color difference signals, R-Y and B-Y [9].

The implementation converts the digital color image's (0 - 255) valued R, G, B components to (0 - 255) valued Y, C_b, C_r components using the following transformation.

$$\begin{bmatrix} Y \\ C_b \\ C_r \end{bmatrix} = \begin{bmatrix} 0.299 & 0.587 & 0.114 \\ -0.169 & -0.331 & 0.5 \\ 0.5 & -0.419 & -0.081 \end{bmatrix} \begin{bmatrix} R \\ G \\ B \end{bmatrix} + \begin{bmatrix} 0 \\ 128 \\ 128 \end{bmatrix} \quad \dots(10)$$

The resulting YC_bC_r space is also referred to as the YC_bC_r space.

At the end of this preprocessing the image will be in the form of $YCbCr$ space and ready for further processing compression. The inverse color transformation from the $YCbCr$ space to the RGB space is given by [10].

$$\begin{bmatrix} R \\ G \\ B \end{bmatrix} = \begin{bmatrix} 1.0 & 0.0 & 1.402 \\ 1.0 & -0.344 & -0.714 \\ 1.0 & 1.772 & 0.0 \end{bmatrix} \left(\begin{bmatrix} Y \\ C_b \\ C_r \end{bmatrix} - \begin{bmatrix} 0 \\ 128 \\ 128 \end{bmatrix} \right) \quad \dots(11)$$

In order to give a demonstration on the change of the image Figure (3) gives this comparison of RGB space and $YCbCr$ space.

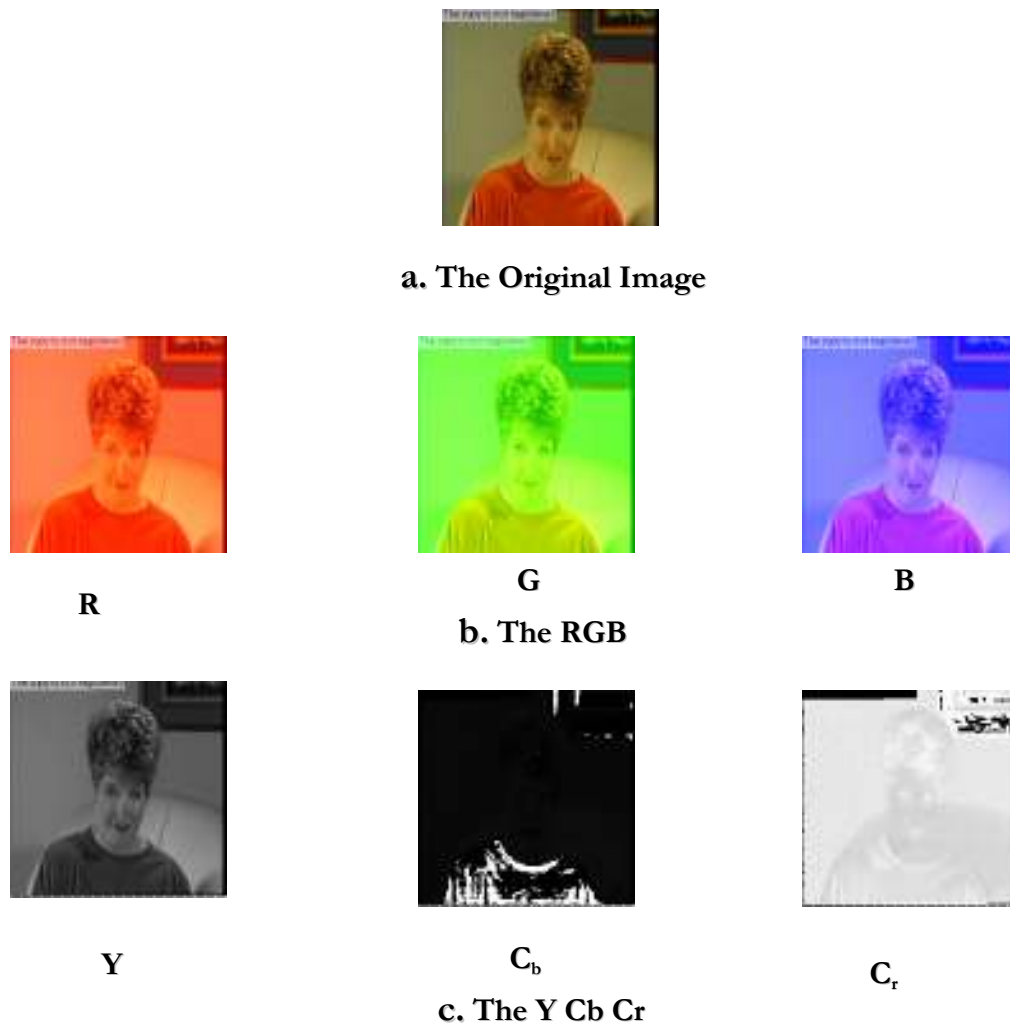


Figure (3) Conversion of RGB into YCbCr

2- The Application of Hybrid Transform

A hybrid transform is applied namely the Ridgelet Transform). In what follows are the details of application of this transform.

2.1 The Ridgelet Transform Computation

This transform is computed using the following procedure and its flowchart is given in Figure (4)

The steps of our methods are

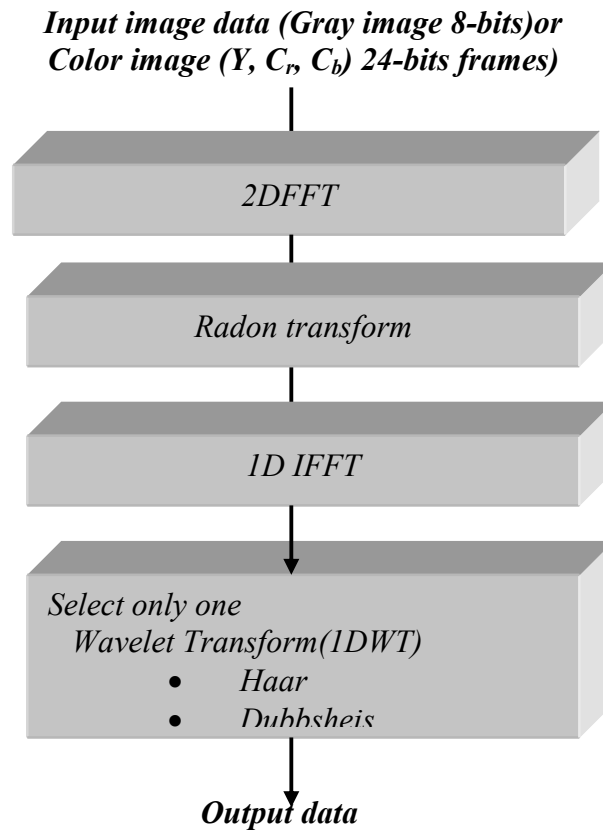


Figure (4) Block Diagram of Ridgelet Transform

It requires first the computation of fast Fourier transform (2DFFT) Next, it requires the application of radon transform. After that the data will be treated as one dimensional information hence, the 1D inverse fast Fourier transform (IFFT) will be applied. The Ridgelet computation requires further the application of 1-D wavelet transform to the resultant data. The final coefficient obtained from the previous step will be called the Ridgelet coefficients. These in turn require the following main steps:

Ridgelet steps are as follows

1. Cartesian to polar conversion use an interpolation scheme, which requires the substitution of the sampled values of the Fourier transform, where the points fall on lines through the origin.

2. Perform the one-dimensional Inverse Fast Fourier Transform (IFFT) on each line; i.e., for each value of the angular parameter.
3. The (IFFT) is calculated along each radial line followed by a 1D wavelet transform which uses this strategy in connection with Ridgelet transform.

1.2 The Coding Algorithm

The first step of any coding process is the quantization. The proposed quantization schemes applied to the wavelet transform The: Ridgelet transform and the SPIHT coding. This mainly requires the quantization of the significant coefficients using the following equation (12) and dequantization equation (13)

$$Q_v = \text{round integer} \left(\frac{v - \min}{\max - \min} \left(\binom{Nb}{2-1} \right) \right) \quad \dots\dots(12)$$

$q = \text{quantization}$

where

$Nb = \text{number of bit quantization coefficients } (0 - 4).$

$Q_v = \text{quantization output value of image data.}$

$v = \text{real input value of image data..}$

$\min = \text{min value of transform .}$

$\max = \text{max value of transform..}$

$D_v = \text{decontization}$

$$D_v = \frac{Q_v (\max - \min)}{\binom{Nb}{2-1}} + \min \quad \dots\dots(13)$$

1.3 Quantization Using SPIHT

The quantization method that is used to generate in this study is the SPIHT. It is expected to achieve good performance by exploiting the spatial dependencies of pixels in different sub-band of scalar wavelet transform. The SPIHT coder is chosen after several experiments in this thesis due to its good objective and computational performance. This section gives the operational ideas behind SPIHT and a method for improving its performance for wavelet and multiwavelet compression methods.

The SPIHT algorithm is adopted here from which uses partitioning the pixel value into parent-descendent group. The coder starts with a threshold value that is the largest integer power of two that do not exceed the largest pixel value. Pixels are evaluated in turn to see if they are larger than the threshold; if not, these pixels are considered insignificant. If parents and all of its descendents are insignificant, then the coder merely records the parent's coordinates. Since the children coordinates can be inferred from those of the parents, those coordinates are not recorded, resulting in a potentially great savings in the output bit stream. After locating and recording all

the significant pixels for the given threshold, the threshold is reduced by factor of two and the process is repeated. By the end of each stage, all coefficients that have been found to be significant will have their most significant bit (when considered as binary integers)

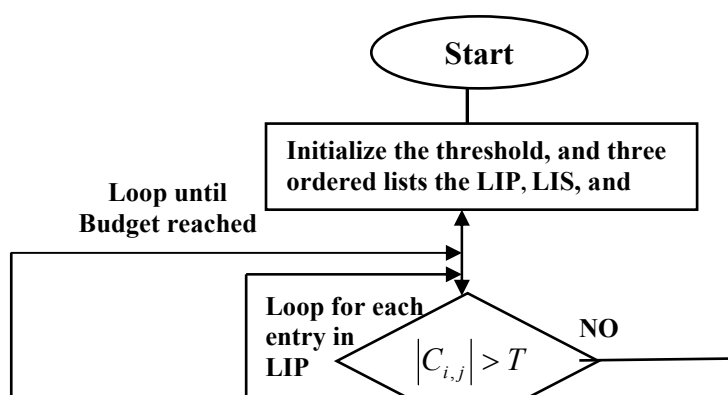
recorded. As further passes occur, more precision is added to the value stored for each pixel. In this manner, the SPIHT algorithm performs a rough sorting of pixel values by magnitude and records their values one bit at a time. It is this separation of bit planes that makes SPIHT an embedded coder: at any point in the output data stream, only the most significant bits for any given pixel are transmitted.

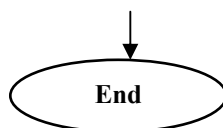
2.4 In order to implement such algorithm the listed abbreviation will be used in its procedure:

- LIP: List of Insignificant Pixels (individual insignificant coefficients),
- LIS: List of Insignificant Sets (insignificant coefficient trees and sets),
- LSP: List of Significant Pixels (significant coefficients).

This algorithm will result in two types of tree which are:

- Type A- checks all descendants for significance,
- Type B-checks all the descendants with the exception of the immediate children. This algorithm is given as flowchart in Figure (5).





2.5 The Application of SPIHT Coding Technique Using Ridgelets Coefficients.

The SPIHT algorithm is a very useful tool for uniformly quantizing the coefficients obtained from the wavelet sub band decomposition of images. The following coding technique for the proposed images with straight singularities is very effective in overcoming the shortcomings of the wavelet transform based coding methods when applied to images with linear edges. The technique is as follows: shown in Figure (6)

1. Represent the image data as intensity values of pixels in the spatial Coordinates.
2. Apply the Ridgelet Transform on the image matrix and get the Ridgelet coefficients of the image.
3. Quantize the available coefficients) and apply the SPIHT algorithm .
4. Use any form of Huffman coded on the bit stream available from the SPIHT encoder.

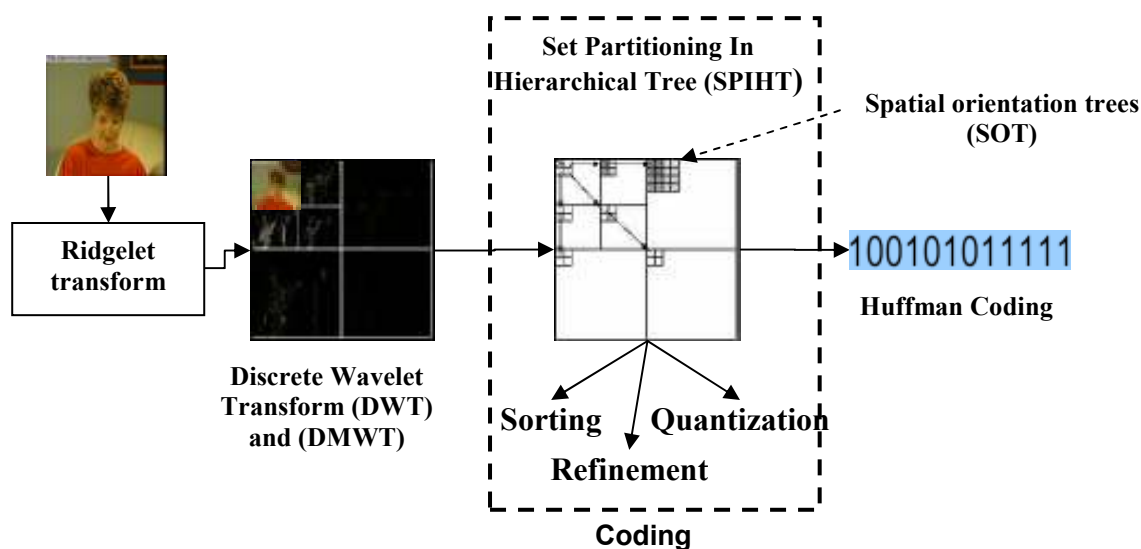


Figure (6) The image encode steps

3 Application of the RLC and Huffman Coding

To compress the image saves the low pass data as it is and does a run length encoding of the rest. Before entering the run length encoding phase it needs to bring the entire near zero coefficients to exactly zero. Otherwise the run length encoding will not be very successful. By dividing the coefficients by some number, all the near zero coefficients turn in to true zeros, and the run length encoding can start, each coefficient is translated into a symbol whose (msb) most significant bit describes what type of symbol it is. If the bit is 0, the rest of the bits in the symbol describe the coefficient value. If the bit is 1, the rest of the bits describe the number of zeroes before the next coefficient. To encode these symbols as well as possible, Huffman encoding is used after you introduce as few symbols as possible. After the Huffman encoding you get the small Huffman code. This is saved here in the implemented software to a file together with Huffman lookup table and low pass data.

Image Video Compression:

The 16- frame color video images of Mom shown in Figure (7) used itself color image 24- bit for 16- frames only of size $(128 \times 128 \times 24bit)$., on which wavelet- based compression methods are known to work well. Performance of different wavelet and

multiwavelet methods changes significantly when "synthetic" test images is used. The experimental facility to get the test image and the data acquisition are briefly described

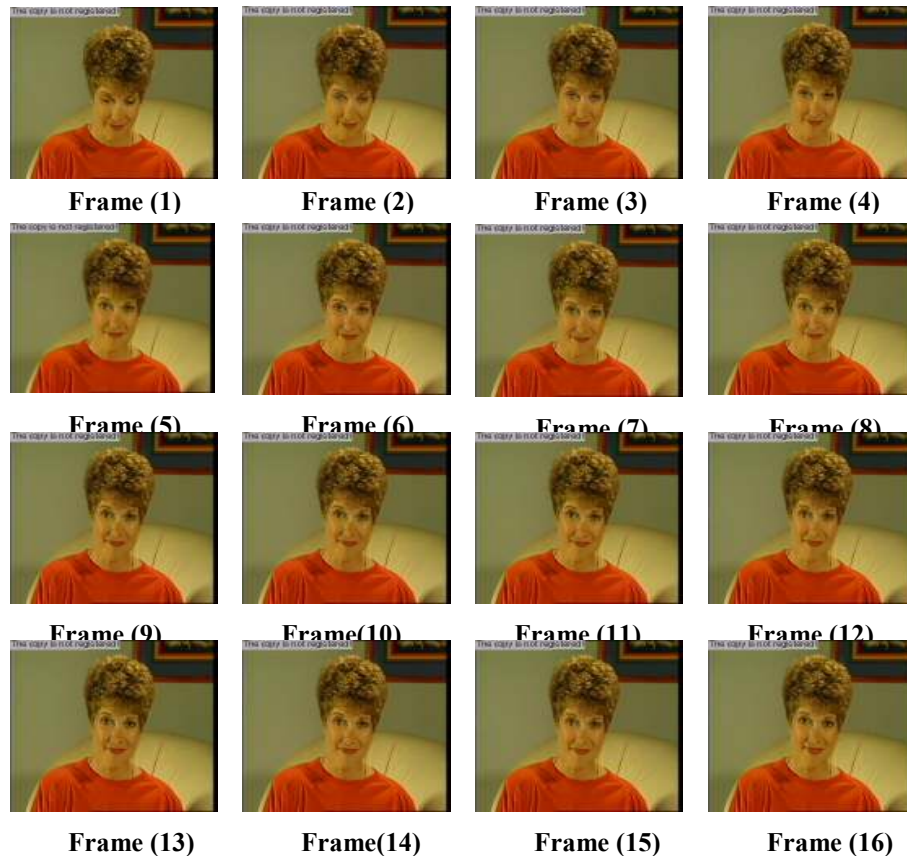


Figure (7) Mom image sequence 16- frame size each one $(128 \times 128 \times 24bit)$

Simulation Results of Image Video Compression:

Objective results given in the next section are provided of eqs

$$PSNR = 20 \log_{10} \left(\frac{255}{RMSE \text{ error}} \right) dB \quad \dots\dots\dots(14)$$

$$RMSE = \sqrt{\frac{1}{N \times M} \sum_{x=0}^{N-1} \sum_{y=0}^{M-1} \left(I(x, y) - \hat{I}(x, y) \right)^2} \quad \dots\dots\dots(15)$$

to determine the (PSNR) value. Since all tests here are performed on 8-bit grayscale and 24-bit color images, for each images, a number of wavelet and multiwavelet filters are tested and the compression.

ratio and bit rate which are varied to quantization value. Some compression parameters, such as the decomposition depth for a particular type of transform, have fixed values and are mentioned now so that such details can be omitted later.

Multiwavelet was used to implement the compression process. The algorithm is applied to image (MOM) with 3-level of variance. Since the estimated variance field has the characteristic of the image CR. Next, the SPIHT coder is applied in to achieve the compression of the variances transform. From the PSNR results that are computed for all the experiments performed, it is observed that both methods yield comparable result. The

relationship between PSNR & Bitrate, Bitrate & Quantization value using eqs (13) and (14), time & Quantization value are also plotted.

- Figure (8) indicate the relation between B_r and Q_v , that the closeness and constitution the resulted of DB4 Ridgelet and MWT SPIHT curves where B_r values decreases gradually. About Haar Ridgelet and MWT SPIHT there is great space between them and the previous curves. There is also a gradual decrease in B_r values with increase in Q_v and finally Haar SPIHT and DB4 SPIHT. Results are constant as observed in the whole track for the value of $B_r=0.1$.
- In Figure (8) it can be seen that the curve for MWT and the Ridgelet gives high B_r values which decrease gradually with Q_v values. Curves for Haar Ridgelet MWT SPIHT and DB4 Ridgelet are reduced gradually with increasing Q_v . Haar SPIHT and DB4 SPIHT are almost constant for the value of $B_r=0.09$. Previous discussions are valid for all cases of different frame numbers of 8-12-16 frames.
- The relation between B_r and Q_v for various numbers of frames using Haar Ridgelet can be seen as consistency of curves for the cases of $N=1, 2$ and 3 as shown in Figure (9).
- By using Haar SPIHT, one can conclude that a consistent curve and great reduction in B_r values are achieved in comparison with the previous case. The observed curves are similar in case of $N=2$ and in case of $N=3$ as shown in Figure (10).

Conclusion:

In this research the first two hybrid transform structure is implemented and tested. Several examples were carried out to verify the this structure which has achieved an excellent performance in image compression.

Some flashing remarks can be concluded .

1. Hybrid coefficients offer benefits over all separable methods in terms of scattered and high pass coefficients. This is because it is less sensitive to coefficient reduction and thus gives a better quality of the image for compression process.
2. Using a hybrid scheme ensures, the same original image dimensions. At the same time it minimizes the redundancy for data compression application.
3. General remarks can be written about the proposed hybrid transform compression method:
 - Hybrid coefficients require fewer bits of the individual transforms.
 - These can further decrease bit rate by increasing the values of the quantization.
 - The ability to adapt the quality of the required bit rats through the use of the quantization value.
 - A quantization value of orders 4-16 represents a good compromise between quality and compression.
 - Hybrid transform requires shorter time than individual transforms.

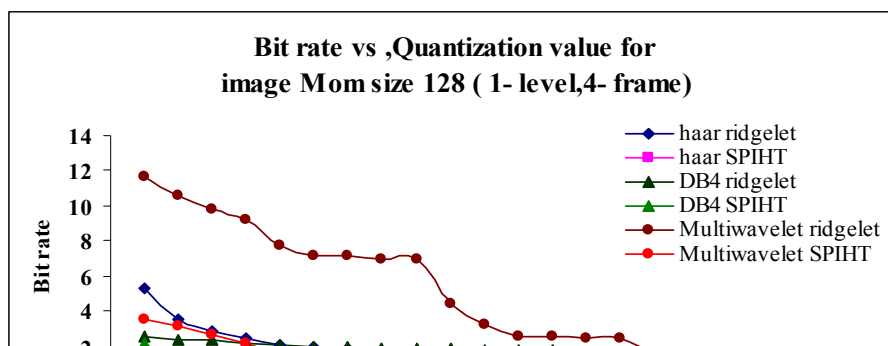
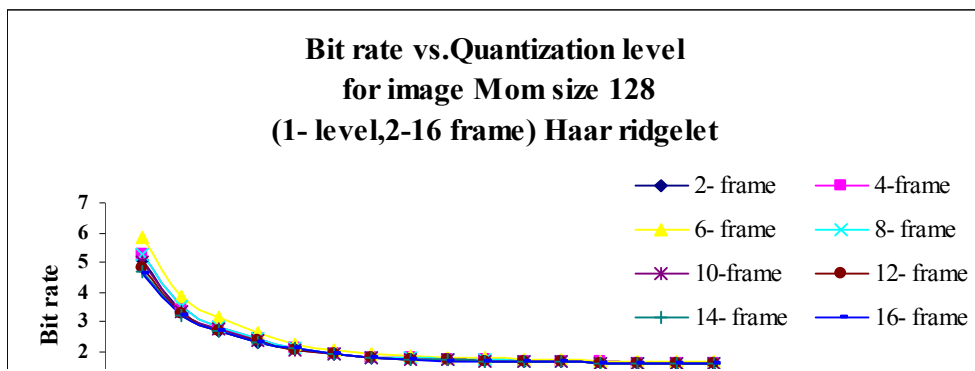


Figure (8 a, b, c) Bit rate & quantization value for image mom (1,2,3-level,4 frame) respectively.



Reference:

1. Njaa. H "Connection between the need for compression, bandwidth and quality for multimedia transmissions in UMTS" M.Sc. Thesis, University College Faculty of Engineering and Science Grimstad, May 2004.
2. Hong, E. S. . Ladner R.E, "Group Testing for Image Compression", IEEE Transactions on Image Processing, vol. 11, pp. 901-11, August 2002
3. Subhasis Saha "Image Compression - from DCT to Wavelets: A Reviewby" ACM Crossroads Student Magazine The ACM's First Electronic Publication, © Copyright 2000-2004 by ACM, Inc. Location: www.acm.org/crossroads/xrds6-3/sahaimgcoding.html
http://164.214.2.51/ntb/2002SICS/Comp_Tutorial_Apr02_pt2.PDF
4. Neelamani.R., Queiroz.R, Fan.Z, Dash.s,& Baraniuk,R "JPEG Compression History Estimation for color images" 2001.
5. Sagwine S.J, Horne R.E.N "colour image processing", Landon, Chapman and Hall 1998.
6. Berts. J& Persson. A "Objective and subjective quality assessment of compressed digital video sequences" M.Sc. Thesis University of Technology Göteborg, Sweden, 1998.
7. Strela .V. and Walden .A.T., "orthogonal and Biorthogonal Multiwavelet for signal denoising and image compression" Image Processing. pp96-107, 1998.
8. Mahamod.W.A.,& Abdulwahab. M.S., and H.N.AL.Taai, "The determination of 3D Multiwavelet transform" IJCCCE, VOL2, No.4, 2005.
9. Rout .S., "Orthogonal VS.biorthogonal wavelets for image compression", M.SC. Thesis, Virginia Polytechnic Institute and State University, Blacksburg, Virginia Polytechnic , August 21, 2003.
10. Bauschke H. H., Hamilton C. H. . Macklem, M. S. McMichael, J. S, and. Swart N. R, "Recompression of JPEG images by requantization," IEEE Trans. Image Processing, vol. 12, pp. 843–849, Jul. 2003.